

## General Disclaimer

### One or more of the Following Statements may affect this Document

- This document has been reproduced from the best copy furnished by the organizational source. It is being released in the interest of making available as much information as possible.
- This document may contain data, which exceeds the sheet parameters. It was furnished in this condition by the organizational source and is the best copy available.
- This document may contain tone-on-tone or color graphs, charts and/or pictures, which have been reproduced in black and white.
- This document is paginated as submitted by the original source.
- Portions of this document are not fully legible due to the historical nature of some of the material. However, it is the best reproduction available from the original submission.

NGR-59-009-015

DYNAMIC ADSORPTION OF CARBON DIOXIDE ON MICROPOROUS CARBONS

O. P. Mahajan, M. Morishita\* and P. L. Walker, Jr.

The Pennsylvania State University  
Materials Science Department  
University Park, Pennsylvania

NG-50-173

(ACCESSION NUMBER) 30

(PAGES) 30

CA-165525

(NASA CR OR TXR OR AD NUMBER)

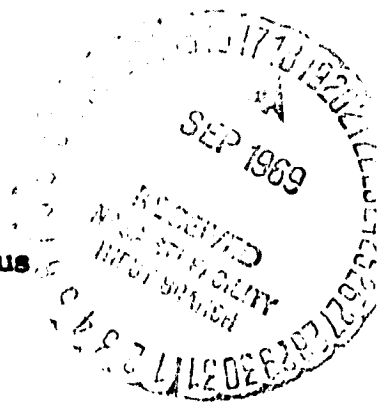
(THRU)

(CODE) 96

(CATEGORY)

FACILITY FORM 608

The dynamic adsorption of CO<sub>2</sub>, at a partial pressure of about 4 Torr (total pressure, 1 atmosphere), has been studied on two relatively pure carbon sieves and one commercial active carbon at 25°C. Regeneration of the carbon activity over a number of adsorption-desorption cycles has also been studied. The capacity of the carbon for CO<sub>2</sub> and its regeneration depends not only upon the porous nature of the carbon but also on the amount and type of the impurities present on the carbon surface. The results show that a substantial proportion of CO<sub>2</sub> adsorbed on the active carbon is held on impurities, the carbon with its large surface area acting as a support for these impurities.



1. INTRODUCTION

Control of atmospheres in space vehicles is a major concern. For short space missions, undesirable contaminants, like CO<sub>2</sub>, are recovered and dumped. For long space missions, a regenerable system where CO<sub>2</sub> is converted back to a desirable constituent of the atmosphere is mandatory.

An adsorption process for the recovery of CO<sub>2</sub> from the atmosphere is strongly being considered. Synthetic zeolite molecular sieves are strong contenders for CO<sub>2</sub> recovery for both short and long space missions (1). In dry atmospheres, they have greater capacity for CO<sub>2</sub> than do activated carbons (2,3). However, space vehicles contain moisture; and since the zeolites have a greater affinity for water than for CO<sub>2</sub>, their capacity for CO<sub>2</sub> is quickly reduced through water uptake. Major et al (2) have studied the dynamic adsorption of CO<sub>2</sub> (0.5% in air) from a wet stream by zeolites and a number of commercial active carbons. They studied the effect of cycling, where adsorption is continued for 1 hr and

\*On leave from the Nippon Carbon Company, Ltd., Japan

desorption of the bed (by evacuation) is conducted for 15 min at room temperature. They find that the zeolite sieve has the greater capacity for the first four cycles; however, for additional cycles the active carbon is clearly superior. The active carbon was cycled 300 times without any loss in CO<sub>2</sub> adsorption capacity.

Recently, a number of carbon molecular sieves (CMS) have been prepared in this laboratory (4-6). The CMS have most of their pores in the 4-7 Å range, compared to relatively larger pores present in commercial active carbons. The sieves are potentially of interest in adsorbing CO<sub>2</sub> because of their smaller pores; CO<sub>2</sub> would interact significantly with more than one pore wall and thus have a higher heat of adsorption than on active carbon. More adsorption would thus result per unit adsorbent area in the low relative pressure range.

In the present work, the adsorption of CO<sub>2</sub> has been studied at 25°C, both under static and dynamic conditions, on one commercial active carbon and two carbon sieves prepared from Saran 489. In the dynamic adsorption work, CO<sub>2</sub> sorption was studied from a He-CO<sub>2</sub> mixture containing about 0.5% CO<sub>2</sub>, the upper limit considered acceptable in space vehicles for long space missions.

## 2. EXPERIMENTAL

### 2.1 Materials

2.1.1 Activated carbon. Barneby-Cheney medium activated coconut shell charcoal of 4x10 mesh particle size was used. It had 1100 m<sup>2</sup>/g N<sub>2</sub> BET surface area, 0.6 g/cm<sup>3</sup> apparent density, and 1.6% ash content.

2.1.2 Carbon molecular sieves. The two carbon sieves studied were prepared from Saran 489 using 20%, by weight, lignite pitch and 17% coal tar pitch as binders. They are designated as CMS-A and CMS-B, respectively. Details of their preparation have been described elsewhere (6). The two sieves exhibit 4A

molecular sieve properties. That is, they adsorb large quantities of CO<sub>2</sub>, as will be seen shortly, but show only slight uptake of n-butane. The n-butane surface area for the two sieves is only about 20 m<sup>2</sup>/g.

## 2.2. Sorption Studies.

2.2.1. Dynamic adsorption. Twenty grams of the adsorbent was packed into a quartz tube of 3/4 in I.D. The adsorbent bed was held in position between two quartz wool plugs. Before an adsorption run, the bed was heated in He or in vacuo at a given temperature. The bed was then cooled to 25 ± 0.2°C. This temperature was maintained by two air coolers connected through a temperature controlling relay system. The He-CO<sub>2</sub> mixture was dried by passing through an Anhydrone column. Anhydrone has been suggested as being the best drying agent for CO<sub>2</sub> (7). If a wet stream was desired, the mixture was passed through a water bubbler, maintained at 25°C, to introduce 23.7 Torr of water to the stream. The mixture was passed through the adsorbent bed at a flow rate of 300 cc/min. The effluent gas, after drying with Anhydrone, was analyzed by a Gow-Mac Gas Analyzer, Model 20-100, the output signal from which was fed to a 150 AR microvoltmeter-ammeter. The concentration of CO<sub>2</sub> in the effluent stream was monitored as a function of time. Ease of regeneration of the bed was studied in flowing He or H<sub>2</sub>. A number of cycles were run to study possible loss in bed capacity.

2.2.2. Static adsorption. Sorption was followed gravimetrically using a Cahn RG Electrobalance. A sample weight of ca 0.4 g was placed in a quartz bucket, which in turn was suspended from the balance arm by a Pt wire. Before adsorption runs, the sample was outgassed at a given temperature to 10<sup>-6</sup> Torr. The pressure range studied was ca 15x10<sup>-3</sup> Torr to 300 Torr. The extent of adsorption was measured after 30 min; equilibrium was attained within this time. The saturation vapor pressure of CO<sub>2</sub> at 25°C was taken as 63.5 atmospheres (8).

### 3. RESULTS AND DISCUSSION

The effect of recycling on the bed capacity of the medium activated charcoal (referred hitherto as active carbon in the text), originally outgassed at 400°C, is shown in Figure 1. Between each cycle, the bed was regenerated in flowing He at 25°C. The He flow was continued till no CO<sub>2</sub> could be detected in the exit stream; this required about 2 hr. Bed capacities, computed from the graphical integration of the break through curves, are shown in Table I. It is seen that after the first two cycles, the bed capacity decreases only slowly for additional cycles. The bed capacity was restored to its original value after 8 cycles by heating the active carbon in flowing He at 150°C for 6 hr.

Break through curves and data for the two 400°C outgassed carbon sieves are also presented in Figure 1 and Table I. It is seen that both the break through times and bed capacities are significantly less than those for the active carbon. However, unlike the active carbon these values do not change with cycling.

The decrease in the bed capacity of the active carbon on recycling (Table I) cannot be attributed to closure of some of the pores due to CO<sub>2</sub> adsorption, because such a possibility should have been more pronounced in the case of the carbon sieves which contain pores of molecular dimensions. The higher sorption capacity of the active carbon relative to that of the carbon sieves was contrary to expectations, because it was believed that the sieves with their smaller pores will adsorb more CO<sub>2</sub> at the low relative pressure used, that is  $7.9 \times 10^{-5}$ .

In order to check the possibility of whether the lower sorption capacity of the carbon sieves might be due to blocking of some of the pores of the filler carbon by the binder, the two sieves were activated in CO<sub>2</sub> at 800°C to 1.3 and 1.8% burn-off, respectively, in the manner described elsewhere (6). This treatment should have opened any pores blocked by the binder phase. When the results of adsorption on the activated sieves are considered (Table I), it is seen that activation produces only a slight increase in bed capacity.

In order to compare the sorption capacities of the active carbon and the CMS for CO<sub>2</sub> over a significant pressure range, CO<sub>2</sub> isotherms (25°C) were determined on the 400°C outgassed samples. The results are plotted in Figures 2 and 3. It is seen that the active carbon adsorbs more CO<sub>2</sub> than the CMS at lower pressures, whereas at higher pressures the latter are the superior adsorbents.

The sorption results have been plotted according to the Dubinin equation (9):

$$\log V = \log V_0 - D(\log p_s/p)^2$$

where

V = amount adsorbed at equilibrium pressure p

V<sub>0</sub> = micropore capacity

p<sub>s</sub> = saturation vapor pressure of the adsorbate

$$D = 0.434 \frac{BT^2}{\beta^2}$$

where

B = a constant which is a measure of the micropore size

β = affinity coefficient of the adsorbate relative to N<sub>2</sub> or benzene

The values of V<sub>0</sub> and slopes of the linear regions of the plots for the active carbon and carbon sieves are given in Table II. A very good straight line relationship is obtained for the carbon sieves over the entire pressure range studied (cf. Figure 4). However, in the case of the active carbon (Figure 5), a linear relationship is observed only below  $(\log p_s/p)^2 = 10$ . For larger values, sorption volumes lie above the extrapolated straight lines. The lower limit of the applicability of the Dubinin equation is  $V/V_0 = 0.05$  (10). In the case of the active carbon, this limit is seen to be significantly higher. The authors feel that this is probably due to significantly higher adsorption energies for the initial amounts of CO<sub>2</sub> adsorbed on the active carbon sample. That such a conclusion is justified will become evident shortly.

In the case of microporous adsorbents the micropore capacities determined from the  $\text{CO}_2$  isotherms at  $25^\circ\text{C}$  can be used to estimate surface areas (11-13). The surface areas of the three samples, using  $25.3\text{A}^2$  for the molecular area of  $\text{CO}_2$  (14), are given in Table II. They are found to vary in the order: CMS-A > active carbon > CMS-B. Although the surface area of the active carbon is less than that of CMS-A, the former adsorbs more  $\text{CO}_2$  at lower pressures (Figure 2).

When the results for the active carbon are considered, it is surprising to note that even though the Dubinin plot indicates higher adsorption energies for the initial amount of  $\text{CO}_2$  adsorbed the value of  $D$ , which is inversely proportional to the heat of adsorption, is higher for the active carbon than for the carbon sieves. A higher value for the slope of the Dubinin plot would lead to the prediction of somewhat less adsorption for the active carbon, at least at low pressures (15).

It has recently been shown by Mahajan and Walker (15) that at low pressures the CMS take up at least comparable amounts of Kr relative to the active carbons; at higher pressures the active carbons are the better adsorbents. Lamond and Marsh (11) have also reported that upon increasing the extent of activation of a polyfurfuryl alcohol carbon (which results in enlarging the pore size), the extent of  $\text{CO}_2$  adsorption at lower pressures decreases, although the surface area of the sample increases. At higher pressures adsorption varied in the same order as the surface area. In the light of the above observations, it was expected that the dynamic adsorption of  $\text{CO}_2$  would be greater on the CMS than the active carbon.

It appears that the disparity in the trend of the present results relative to those of Kr adsorption (15) is probably due, at least in part, to different forces involved in the sorption of the two adsorbates on the same type of adsorbents. Since Kr is a non-polar isotropic molecule, its adsorption should

involve only van der Waals dispersive forces. However, the  $\text{CO}_2$  molecule has a quadrupole moment. Beebe et al (16) have reported that the polar centers due to oxygen sites on the carbon surface may interact with the quadrupole associated with the  $\text{CO}_2$  molecule and result in higher uptake of the adsorbate. These workers argue that the non-polar  $\text{CO}_2$  molecule in the adsorbed state, and particularly in the field of polar centers, may behave like a molecule with a permanent dipole. Deitz et al (17) have also reported that the amount of  $\text{CO}_2$  adsorbed per unit area of surface and its heat of adsorption increase with the fraction of the carbon surface covered by hydroxyl groups.

In order to check on the possibility of whether a stronger interaction of  $\text{CO}_2$  with surface-oxygen complexes is responsible for the enhanced adsorption of the active carbon at lower pressures, the dynamic adsorption of  $\text{CO}_2$  was measured after heat treatment in flowing He or  $\text{H}_2$  at increasing temperatures from 400 to 900°C. The soak time at the final temperature for each treatment was 6 hr. The break through curves are plotted in Figure 6. The amount of  $\text{CO}_2$  adsorbed per gram of adsorbent in each run is also given. It is seen that an increasing temperature of heat treatment enhances the uptake of  $\text{CO}_2$ , the uptake increasing from 2.06 cc/g for the 400°C heat-treated sample to 4.18 cc/g for the 900°C heat-treated sample. It is also seen that heat treatment in  $\text{H}_2$  at a given temperature is more effective in increasing the adsorption of  $\text{CO}_2$  than is heat treatment in He. With increasing heat treatment temperature, removal of surface-oxygen complexes (if present) would be more complete. Thus, enhanced  $\text{CO}_2$  adsorption cannot be attributed to greater amounts of oxygen complex. Obviously some other explanation must be sought.

The sorption isotherm on the 900°C outgassed active carbon (Figures 2 and 3) gave a larger amount of  $\text{CO}_2$  adsorbed over the entire pressure range than that for the 400°C outgassed active carbon and the CMS. The Dubinin plot gives the same value of  $V_0$  as for the 400°C outgassed sample (Table II), suggesting



that the enhanced uptake of  $\text{CO}_2$  cannot be attributed to a change in the pore structure of the carbon as a result of heating at  $900^\circ\text{C}$ . A comparison of the Dubinin plots for the  $400$  and  $900^\circ\text{C}$  outgassed samples (Figure 5) shows that below  $(\log p_s/p)^2 = 10$ , sorption on the latter is associated with higher adsorption energies. The higher adsorption energy for the  $900^\circ\text{C}$  outgassed sample is also indicated by a smaller value of the slope for the linear region of the Dubinin plot (Table II).

The effect of recycling on the bed capacity of the  $900^\circ\text{C}$  outgassed active carbon, when adsorption is studied from a dry stream, is shown in Figure 7. The bed capacities computed from graphical integration of the break through curves are given in Table I. It is seen that the bed capacity decreases sharply after the first cycle. The decrease continues, though less sharply, for subsequent cycles up through the fourteenth, where the value has dropped to  $1.38$  cc/g. For subsequent cycles, the bed capacity remains unchanged.

It is interesting to note that although either outgassing or heat treatment in He at  $900^\circ\text{C}$  results in the same bed capacity (Figure 6 and Table I), the shapes of the break through curves in the two cases are different (Figures 6 and 7).

The effect of cycling in the case of a wet  $\text{CO}_2$ -He stream is shown in Figure 8 and Table I. In the first cycle, it is seen that following break through the outlet concentration of  $\text{CO}_2$  climbs to a value which exceeds the inlet concentration for a short period. It appears probable that water displaces some of the adsorbed  $\text{CO}_2$ . Water markedly affects the adsorption capacity of the sample. For instance, the bed capacity for the first cycle is  $3.48$  cc/g compared to  $4.17$  cc/g for the dry stream. Furthermore, the bed capacity becomes constant after only four cycles or when the amount of  $\text{CO}_2$  adsorbed equals  $1.77$  cc/g. This amount is significantly greater than the constant value finally attained after fourteen cycles for the dry stream.

In order to study the ease of regeneration and, hence, the stability of adsorbed  $\text{CO}_2$ , the active carbon bed after the seventeenth cycle (in the dry stream studies) was heated in flowing  $\text{H}_2$  at increasing temperatures. The soak time for each treatment was 6 hr. The dynamic adsorption of  $\text{CO}_2$  was measured after each heat treatment. Hydrogen was specifically chosen for this study because there is interest, in the space program, in reacting  $\text{CO}_2$  and  $\text{H}_2$  over a nickel catalyst to produce water, which can then be electrolytically dissociated to  $\text{O}_2$  and  $\text{H}_2$ . The bed capacities for each heat treatment are given in Table III. It is seen that the adsorbed  $\text{CO}_2$  is fairly stable; its desorption does not start at  $100^\circ\text{C}$ . Increasing amounts of  $\text{CO}_2$  are desorbed between  $200\text{--}400^\circ\text{C}$ . Between  $400\text{--}600^\circ\text{C}$  heat treatment, the bed capacity remains essentially constant. However, following heat treatment at  $700^\circ\text{C}$  there is a slight, though significant, decrease in bed capacity. It may be mentioned that when He was used for regenerating the bed, the bed capacity monotonically increased with increasing temperature of heat treatment. It appears likely that the decrease when  $\text{H}_2$  is used is due to its chemisorption at some of the 'active' sites on the carbon surface which otherwise would have been involved in the adsorption of  $\text{CO}_2$ . Chemisorption of  $\text{H}_2$  is known to occur on graphite (18-20), charcoals (21,22) and graphitized carbon blacks (23).

Since above  $700^\circ\text{C}$   $\text{H}_2$  causes gasification of carbon to give methane (23), heat treatment in  $\text{H}_2$  was not carried out at higher temperatures. Instead, above  $700^\circ\text{C}$ , regeneration of the bed was studied in flowing He. It is seen (Table III) that there are slight increases in the bed capacity following heat treatment at  $800$  and  $900^\circ\text{C}$ . The sample was then outgassed at  $900^\circ\text{C}$  for 72 hr. Even after this drastic treatment, the original bed capacity is not restored, suggesting that a part of the chemisorbed  $\text{H}_2$  is still not desorbed under these conditions. Walker and co-workers (23) have observed recently that  $\text{H}_2$  chemisorbed on a Graphon sample is held very strongly; and its complete

elimination takes place only after outgassing for 72 hr at 1000°C. In the present study, a higher temperature of outgassing was not used so as to avoid the possibility of sintering of the 'active' sites on the porous carbons responsible for CO<sub>2</sub> adsorption.

Since the adsorbed CO<sub>2</sub> is extremely stable, it is evident that it is not held at the carbon surface by mere van der Waals forces. It appears that some chemical or quasi-chemical forces are responsible for the adsorption of that portion of the CO<sub>2</sub> which is not desorbed on H<sub>2</sub> treatment at 100°C. Most likely, the impurity content of the active carbon is interacting with CO<sub>2</sub>. The active carbon used in the present work has an ash content of 1.6%. The major impurity constituents, as determined by qualitative spectrochemical analysis of the low-temperature ashed material, are Si, Fe, Al, Mg, Ca, Na, K; B, Mn and Cu are present as minor constituents. Infra-red analysis reveals the presence of sulfate and nitrate functional groups and silica. The impurities, when present in an appropriate chemically combined form, are capable of interacting chemically with CO<sub>2</sub>. The enhanced uptake of CO<sub>2</sub> with increasing temperatures of heat treatment strongly suggests that the impurities are decomposing thermally or/and are reduced by carbon or CO evolved during the thermal decomposition of surface oxygen complexes, to give products which can react with CO<sub>2</sub>. The latter view is supported by the fact that the bed capacity is significantly greater when the active carbon is heated at 600°C in H<sub>2</sub> than in He (Figure 5). This increase occurs in spite of the fact that H<sub>2</sub> is capable of being chemisorbed on carbon at 600°C.

It has been shown by Puri and co-workers (24,25) that heat treatment of charcoal in flowing H<sub>2</sub> at 600°C eliminates surface complexes to an extent which is observed in vacuo or N<sub>2</sub> at 1000°C. Furthermore, it is known that H<sub>2</sub> is chemisorbed at the same sites as oxygen (19,23). Therefore, enhanced uptake of CO<sub>2</sub> following H<sub>2</sub> treatment cannot be attributed to adsorption on additional sites rendered vacant by the desorption of oxygen complexes.

It has been reported by Emmett and Brunauer (26) that the presence of 1% or so of  $K_2O$  on surfaces of iron synthetic ammonia catalysts significantly enhances the adsorption of  $CO_2$ . For instance, a catalyst containing 1.07%  $K_2O$  adsorbed, at a pressure of 300 Torr, 78% more  $CO_2$  at  $-78^\circ C$  than  $N_2$  at the same pressure at  $-183^\circ C$ . These workers suggest that the surface alkali causes a very rapid chemisorption of  $CO_2$  to occur, in addition to usual physical adsorption. By assuming that each molecule of alkali present on the surface can hold one molecule of chemisorbed  $CO_2$ , they report that for a catalyst containing 1.07%  $K_2O^*$ , the alkali covers about 75% of the catalyst surface.

The fact that in the present study the impurities are adsorbing  $CO_2$  and thus enhancing the extent of adsorption is confirmed when results on the de-ashed sample are considered. The active carbon was de-ashed with a HCl-HF mixture in a boiling water bath. It was washed free of Cl ions with demineralized water. The  $25^\circ C$  isotherms on the  $400^\circ C$  and  $900^\circ C$  outgassed, de-ashed samples are shown in Figures 2 and 3. It is seen that for the same temperature of outgassing, the sorption uptake, over the entire pressure range, is significantly less for the de-ashed material than for the as-received sample. For the de-ashed carbon, the  $900^\circ C$  outgassed sample adsorbs more  $CO_2$  than the  $400^\circ C$  outgassed sample. Moreover, the desorption isotherm on the former shows a small hysteresis loop over the entire pressure range. However, subsequent adsorption on the sample was found to be completely reversible. The higher sorption capacity and the irreversibility of adsorption on the  $900^\circ C$  outgassed sample could be due to the influence of traces of impurities which may still be left in the de-ashed material. In this context, Emmett and Brunauer (26) have suggested that a few hundredths of a percent of alkali oxide can significantly influence the adsorption of  $CO_2$ .

---

\*Although the catalyst initially contained 1.07%  $K_2O$ , the workers report that during the reduction of the catalyst, 55-65% of the alkali had volatilized.

It may incidentally be mentioned that Magnus et al (27) have also reported that de-ashing of a wood charcoal decreases the adsorption of  $\text{CO}_2$ . These workers have attributed the higher sorption capacity of the untreated charcoal to the presence of alkali or alkaline earth oxides on the surface.

Dubinin plots on the de-ashed sample are shown in Figure 5 and the parameters of the equation are given in Table II. It is seen that after the removal of impurities, the plots are linear over a wider pressure range. The slopes of the linear regions of the plots increase after de-ashing, indicating that sorption is now associated with a lower adsorption energy, that is heat of adsorption. The Dubinin plot for the  $400^\circ\text{C}$  outgassed sample is found to be linear above  $V/V_0 = 0.02$ , the lower limit of the applicability of the equation (10). Therefore, it appears that departure from linearity above this limit can be attributed to sorption on sites associated with higher adsorption potentials, an assumption made elsewhere in the paper.

It is noteworthy that although the shape of the isotherms (Figures 2 and 3) and the slopes of the Dubinin plots (Table II) differ for different treatments, the value of the micropore capacity, within the limits of accuracy and reliability of these logarithmic plots, remains constant.

The striking influence of the impurities on  $\text{CO}_2$  adsorption is brought out more clearly when the results of dynamic adsorption on the de-ashed sample outgassed at  $900^\circ\text{C}$  are considered (Figure 9). It is seen that the break through time and the bed capacity are very much less than those for the as-received active carbon sample (Figures 1 and 7, Table I). In the present case, the bed capacity decreases only slightly after the first cycle; the value remains constant thereafter. This slight decrease is consistent with a small amount of irreversibly adsorbed  $\text{CO}_2$  as suggested from static adsorption experiments.

When the results for the wet stream in contact with the de-ashed active carbon are considered, it is seen (Table I) that water has a negligible

influence on the adsorption of  $\text{CO}_2$ . This result is in contrast to the result for the as-received active carbon, where the presence of water affected the dynamic adsorption of  $\text{CO}_2$ . It suggests that water is not competing with  $\text{CO}_2$  for adsorption on carbon sites, but is competing for adsorption on inorganic impurity sites.

The sorption isotherms on the active carbon show (Figures 2 and 3) that the percentage increase in the  $\text{CO}_2$  adsorption, brought about by the impurities, decreases with increasing equilibrium pressure. For instance, when the sorption capacity of the active carbon, both before and after the removal of impurities, is considered at a pressure of 4 Torr (which closely represents the partial pressure of  $\text{CO}_2$  at which the dynamic adsorption has been studied in the present work) it is seen that 1.6% impurities can enhance  $\text{CO}_2$  adsorption by about 300%. At a pressure of 250 Torr, the impurities increase  $\text{CO}_2$  uptake by only 20%. In the light of the present work, it appears that a substantial proportion of  $\text{CO}_2$  adsorbed at low relative pressures on the active carbon is held on impurities and that the active carbon, with its large surface area, acts as a support for these impurities.

It was shown earlier (Table I) that, in the case of CMS-B, activation in  $\text{CO}_2$  to a burn-off of 1.8% results in only a minor increase in adsorption of  $\text{CO}_2$ . It was thought probable that oxygen chemisorbed during the process of activation with  $\text{CO}_2$  might possibly be blocking some of the finer pores. In order to check this possibility, a sorption isotherm on the  $900^\circ\text{C}$  outgassed sample was measured (Figure 10). It is seen that there is a significant increase in the extent of adsorption throughout the pressure range.

The coal tar pitch used as a binder had an ash content of 0.24%. The Saran carbon is relatively very pure. Since 17% of coal tar pitch was used as a binder, the ash content of the resultant sieve would be about 0.041%. In view of the profound influence of impurities on the adsorption of  $\text{CO}_2$  observed

In the present work, enhanced adsorption on the 900°C outgassed sample could be due to the influence of small amounts of impurities. However, when the Dubinin plot is considered, it is seen (Figure 4 and Table II) that, unlike the active carbon, the value of  $V_0$  increases following outgassing at 900°C. The slope of the Dubinin plot and, hence, the adsorption energy remain essentially unchanged on increasing the temperature of outgassing, suggesting that additional  $\text{CO}_2$  is adsorbed in some of the pores which were previously blocked by chemisorbed oxygen.

When the sorption isotherms on the de-ashed active carbon are compared with those on the carbon sieves, it is seen (Figures 2 and 3) that the latter adsorb more  $\text{CO}_2$  than the active carbon throughout the pressure range studied, thus confirming our expectations that the carbon sieves should be better adsorbents than the active carbon.

The effect of recycling on the bed capacity of the as-received active carbon shows (Table I) that the initial capacity, as well as the constant capacity attained after a number of cycles, increases with increasing temperature of outgassing of the sample. In each case, the values are considerably greater than those obtained for the de-ashed sample. It appears, therefore, that on heating at increasing temperatures, the impurities are 'activated' to different extents and that in each case  $\text{CO}_2$  adsorbed on some of the impurities is capable of desorption by He.

Since water decreases the adsorption of  $\text{CO}_2$  on the as-received active carbon, it appears that some of the impurities have a greater affinity for water than  $\text{CO}_2$ , thus leading to preferential adsorption of water. It was observed that the constant value of bed capacity obtained for the wet stream was significantly greater than for the dry stream. The exact mechanism for this behavior is open to speculation, but it may involve absorption of  $\text{CO}_2$  in water.

It is difficult to ascertain the exact nature and composition of the impurities present on the carbon surface and the manner in which they are affected on heating. The impurities distributed on the carbon surface are not expected to have the same chemical characteristics as those of the bulk impurities. Therefore, one cannot suggest with any certainty the exact mechanism for the adsorption of CO<sub>2</sub> on the impurities or the manner in which it will be influenced by water.

#### ACKNOWLEDGMENTS

This study was supported on the NASA sustaining University Research Grant NGR-39-009-015.

#### REFERENCES

1. Anon, Chem. Eng. News, 42, 79 (1964).
2. Major, C. J., Sollami, B. J. and Kammermeyer, K., Ind. Eng. Chem., Process Design and Development, 4, 327 (1965).
3. Walker, P. L., Jr. and Shelef, M., Carbon, 5, 7 (1967).
4. Walker, P. L., Jr., Lamond, T. G. and Metcalfe, J. E., III, Proc. Ind. Carbon and Graphite Conf., Society of Chemical Industry, London, 1966, pp. 7-14.
5. Walker, P. L., Jr., Austin, L. G. and Nandi, S. P., Chemistry and Physics of Carbon, Vol. 2, Edited by P. L. Walker, Jr., Marcel Dekker, Inc., New York, 1966, pp. 257-371.
6. Metcalfe, J. E., III, Ph.D. Thesis, The Pennsylvania State University, 1965.
7. Lang, F. M. and Magnier, P., Chemistry and Physics of Carbon, Vol. 3, Edited by P. L. Walker, Jr., Marcel Dekker, Inc., New York, 1968, p. 142.
8. "Handbook of Chemistry and Physics", 33rd Edition, Chemical Rubber Publishing Company, Cleveland, 1961, p. 1935.
9. Dubinin, M. M., Chem. Rev., 60, 235 (1960).
10. Dubinin, M. M., Chemistry and Physics of Carbon, Vol. 2, Edited by P. L. Walker, Jr., Marcel Dekker, Inc., New York, 1966, p. 99.
11. Lamond, T. G. and Marsh, H., Carbon, 1, 281 (1964).



12. Marsh, H. and Siemieniowska, T., *Fuel*, 44, 355 (1965).
13. Walker, P. L., Jr. and Patel, R. L., *Fuel*, in press.
14. Walker, P. L., Jr. and Kini, K. A., *Fuel*, 44, 453 (1965).
15. Mahajan, O. P. and Walker, P. L., Jr., *J. Colloid and Interface Sci.*, 29, 129 (1969).
16. Spencer, W. B., Amberg, C. H. and Beebe, R. A., *J. Phys. Chem.*, 62, 719 (1958).
17. Deitz, V. R., Carpenter, F. G. and Arnold, R. B., *Carbon*, 1, 245 (1964).
18. Redmond, J. P. and Walker, P. L., Jr., *J. Phys. Chem.*, 64, 1093 (1960).
19. Thomas, W. J., *J. Chim. Phys.*, 58, 61 (1961).
20. Barrer, R. M., *J. Chem. Soc.*, 1256 (1936).
21. Long, F. J. and Sykes, K. W., *Proc. Roy. Soc., (London)* A193, 377 (1948).
22. Barrer, R. M., *Proc. Roy. Soc. (London)* A149, 253 (1935).
23. Bansal, R. C., Vastola, F. J. and Walker, P. L., Jr., unpublished work.
24. Puri, B. R., Kumar, B. and Singh, D. D., *J. Sci. Ind. Res. (India)*, 20D, 366 (1961).
25. Puri, B. R. and Bedi, K. M., *Chem. Ind. (London)*, 1899 (1963).
26. Emmett, P. H. and Brunauer, S., *J. Am. Chem. Soc.*, 59, 310 (1937).
27. Magnus, A., Sauter, E. and Kratz, H., *Z. anorg. allgem. Chem.*, 174, 142 (1928).

TABLE I

## EFFECT OF CYCLING ON BED CAPACITY OF CARBONS

<u>Cycle No.</u>	<u>Bed Capacity</u> <u>cc(NTP)/g</u>
<u>Active Carbon</u> *	
1	2.24
2	2.20
3	2.03
4	1.99
5	1.97
6	1.87
7	1.86
<u>Active Carbon</u> **	
a) <u>Dry Stream</u>	
1	4.17
2	3.08
3	2.83
4	2.64
5	2.45
6	2.32
7	2.22
8	2.07
9	1.89
10	1.83
11	1.61
12	1.50
13	1.48
14	1.38
16	1.40
17	1.42
b) <u>Wet Stream</u>	
1	3.48
3	2.18
4	1.85
5	1.85
6	1.78
7	1.77
<u>CMS-A</u> *	
1	1.26
2	1.25
<u>CMS-A, 1.3% burn-off</u> *	
1	1.39
<u>CMS-B</u> *	
1	1.10
2	1.08
<u>CMS-B, 1.8% burn-off</u> *	
1	1.21

TABLE I (continued)

<u>Cycle No.</u>	<u>Bed Capacity</u> <u>cc(NTP)/g</u>
<u>De-ashed Active Carbon</u> **	
a) <u>Dry Stream</u>	
1	0.96
2	0.90
4	0.90
b) <u>Wet Stream</u>	
1	0.95
2	0.86
4	0.86

\*Initially outgassed at 400°C

\*\*Initially outgassed at 900°C

TABLE II  
PARAMETERS OF THE DUBININ PLOTS AND SURFACE AREAS

<u>Sample</u>	<u>Micropore capacity cc(NTP)/g</u>	<u>Slope x 10<sup>-2</sup></u>	<u>Surface area m<sup>2</sup>/g</u>
<u>Active carbon</u>			
outgassed at 400°C	137	12.61	931
outgassed at 900°C	137	11.68	931
<u>De-ashed active carbon</u>			
outgassed at 400°C	137	13.81	931
outgassed at 900°C	137	13.23	931
<u>CMS-A</u>			
outgassed at 400°C	140	12.43	950
<u>CMS-B</u>			
outgassed at 400°C	127	12.00	863
outgassed at 900°C	140	11.80	950

TABLE III  
REGENERATION OF THE ACTIVE CARBON BED  
FOLLOWING THE SEVENTEENTH CYCLE OF CARBON DIOXIDE ADSORPTION

<u>Regeneration Conditions</u>	<u>Bed capacity cc(NTP)/g</u>
<u>Hydrogen</u>	
100°C	1.45
200	2.09
300	3.21
400	3.61
500	3.70
600	3.64
700	3.52
<u>Helium</u>	
800°C	3.70
900	3.86
<u>Outgassing</u>	
900°C	3.88

#### FIGURE CAPTIONS

1. Effect of recycling on the break through curves of dry CO<sub>2</sub> at 25°C on active carbon and carbon sieves, originally outgassed at 400°C. Active carbon: cycle 1, 0; 2, Δ; 3, □; 6, ∇; 7, ●. CMS-A: cycle 1, ▼; 2, X. CMS-B: Cycle 1, ▲; 2, ■.
2. Sorption isotherms of CO<sub>2</sub> on active carbon and carbon sieves at 25°C. As-received active carbon outgassed at 400°C, 0; 900°C, ●. De-ashed active carbon outgassed at 400°C, ∇; 900°C, ▼; CMS-A, □; and CMS-B, Δ, degassed at 400°C.
3. Sorption isotherms of CO<sub>2</sub> on active carbon and carbon sieves in low pressure region at 25°C. As-received active carbon outgassed at 400°C, 0; 900°C, ●. De-ashed active carbon outgassed at 400°C, ∇; 900°C, ▼. CMS-A, □, and CMS-B, Δ, degassed at 400°C.
4. Dubinin plots for CO<sub>2</sub> adsorption on CMS-B at 25°C.
5. Dubinin plots for CO<sub>2</sub> adsorption on active carbon at 25°C.
6. Effect of heat treatment in He and H<sub>2</sub> at different temperatures on the break through curves of dry CO<sub>2</sub> at 25°C on active carbon. Value given for each curve is total uptake per gram of adsorbent.
7. Effect of recycling on the break through curves of dry CO<sub>2</sub> at 25°C on active carbon, originally outgassed at 900°C.
8. Effect of recycling on the break through curves of wet CO<sub>2</sub> at 25°C on active carbon, originally outgassed at 900°C.
9. Effect of recycling on the break through curves of dry CO<sub>2</sub> at 25°C on de-ashed carbon originally outgassed at 900°C.
10. Effect of outgassing temperature on sorption isotherms of CO<sub>2</sub> on CMS-B at 25°C.

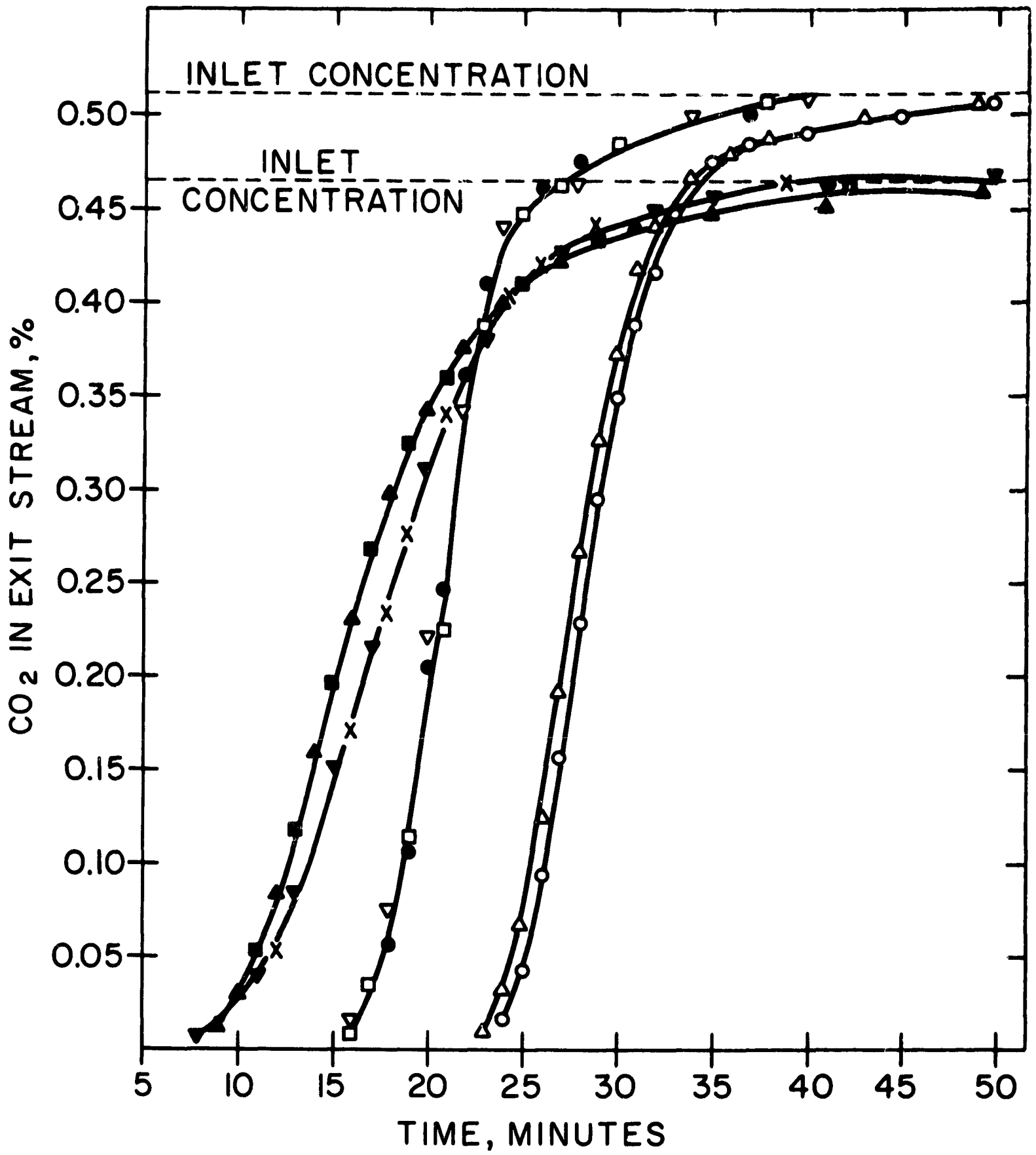


FIG.- I

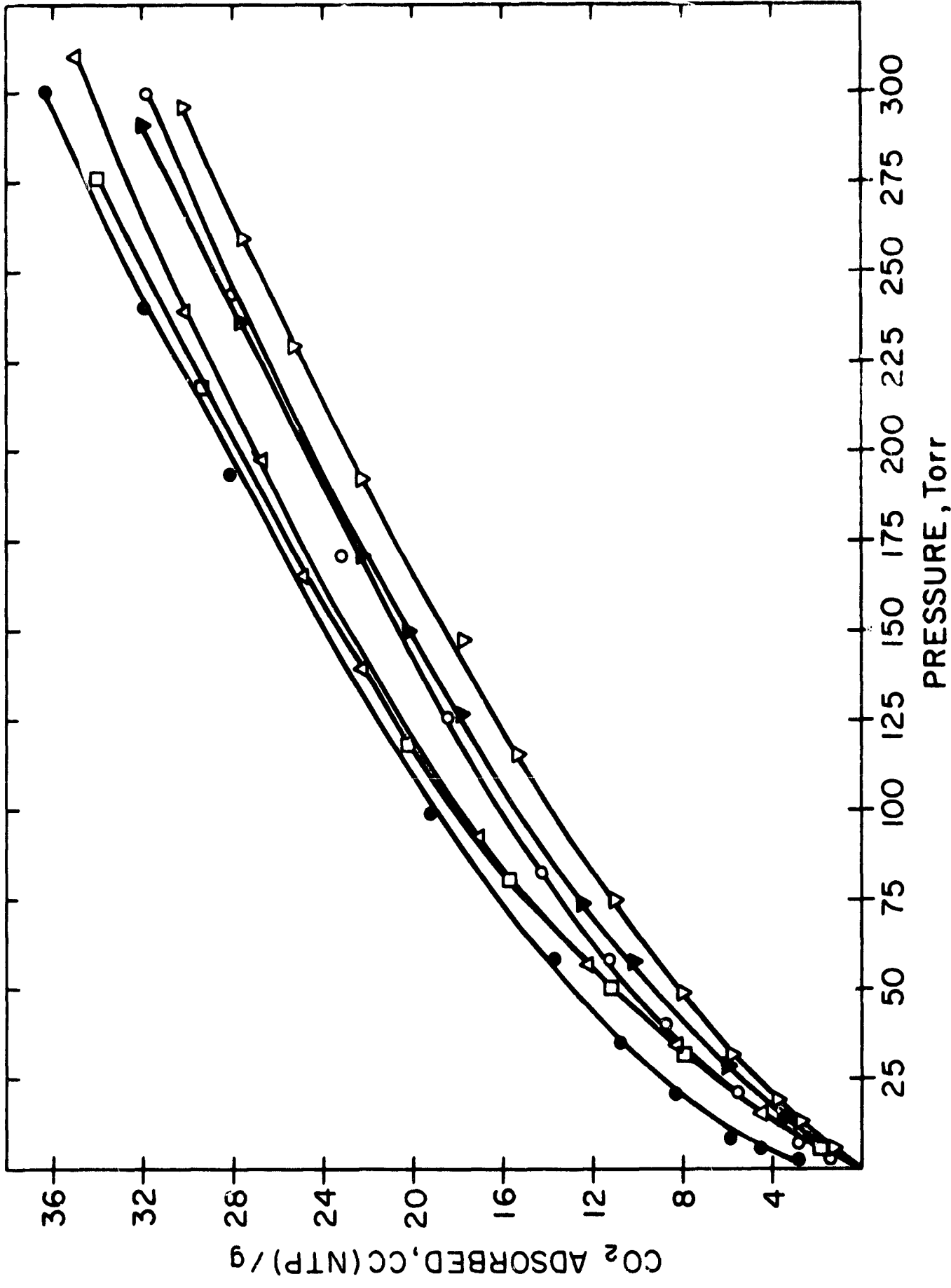


FIG. - 2

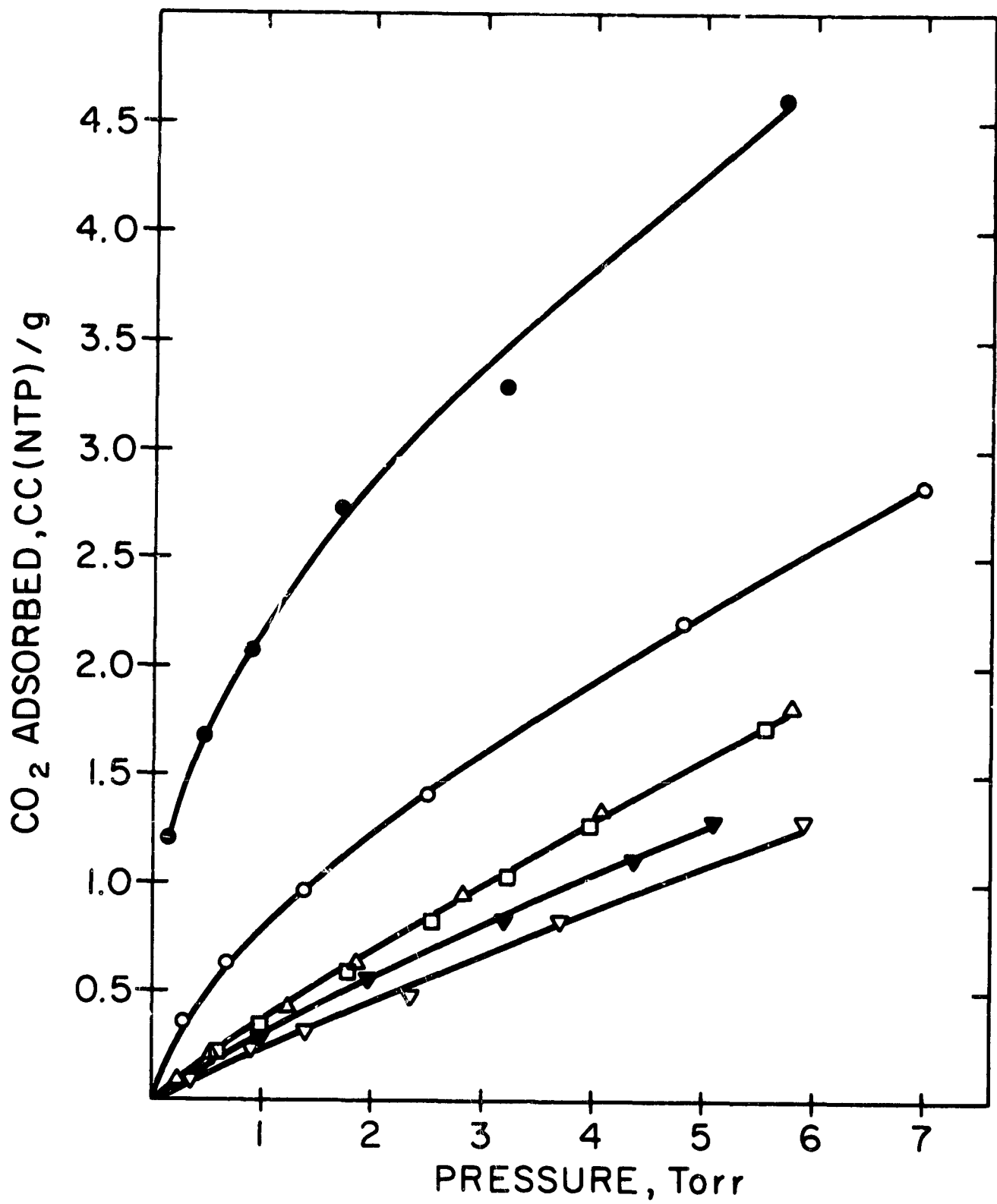


FIG. - 3



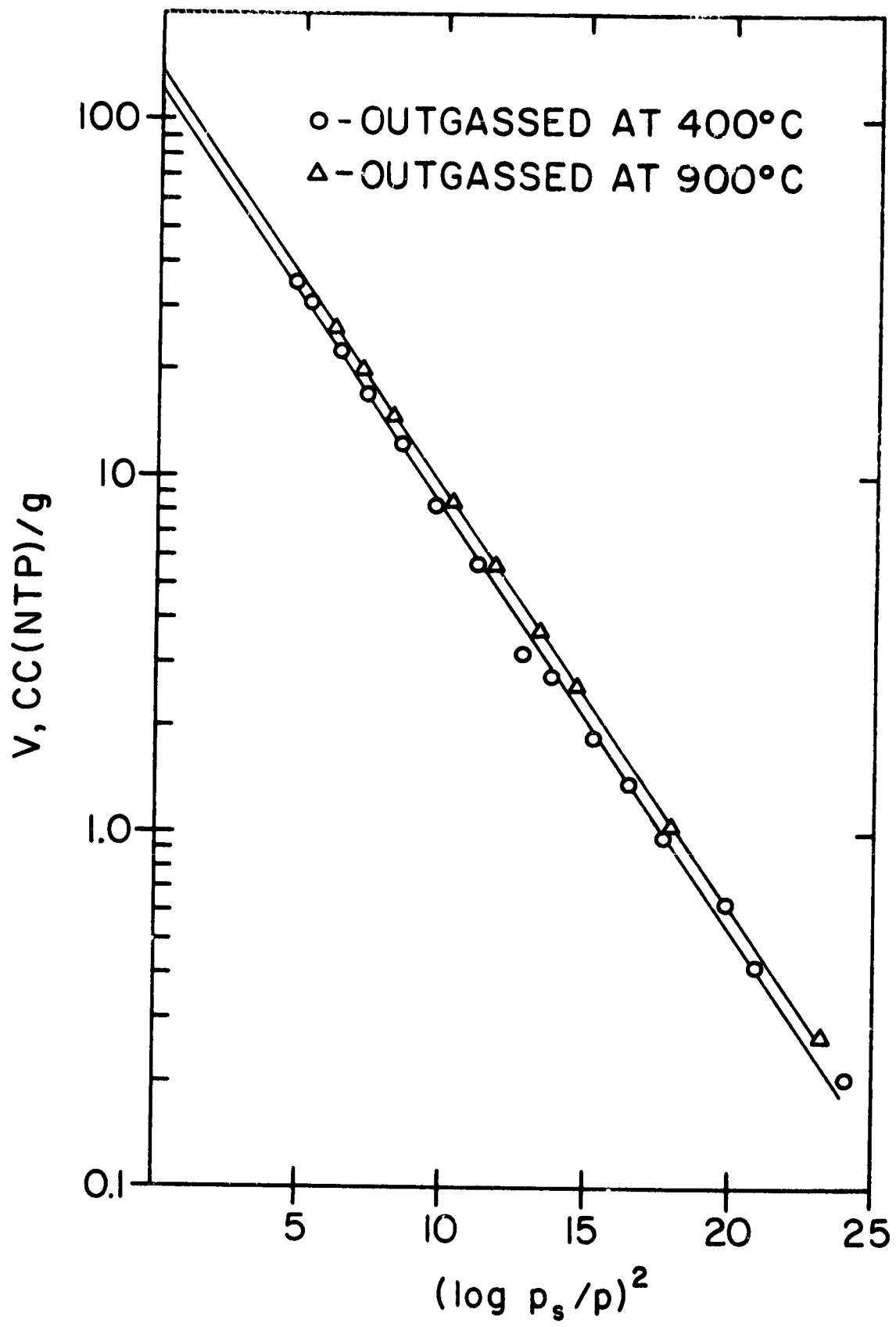


FIG. - 4

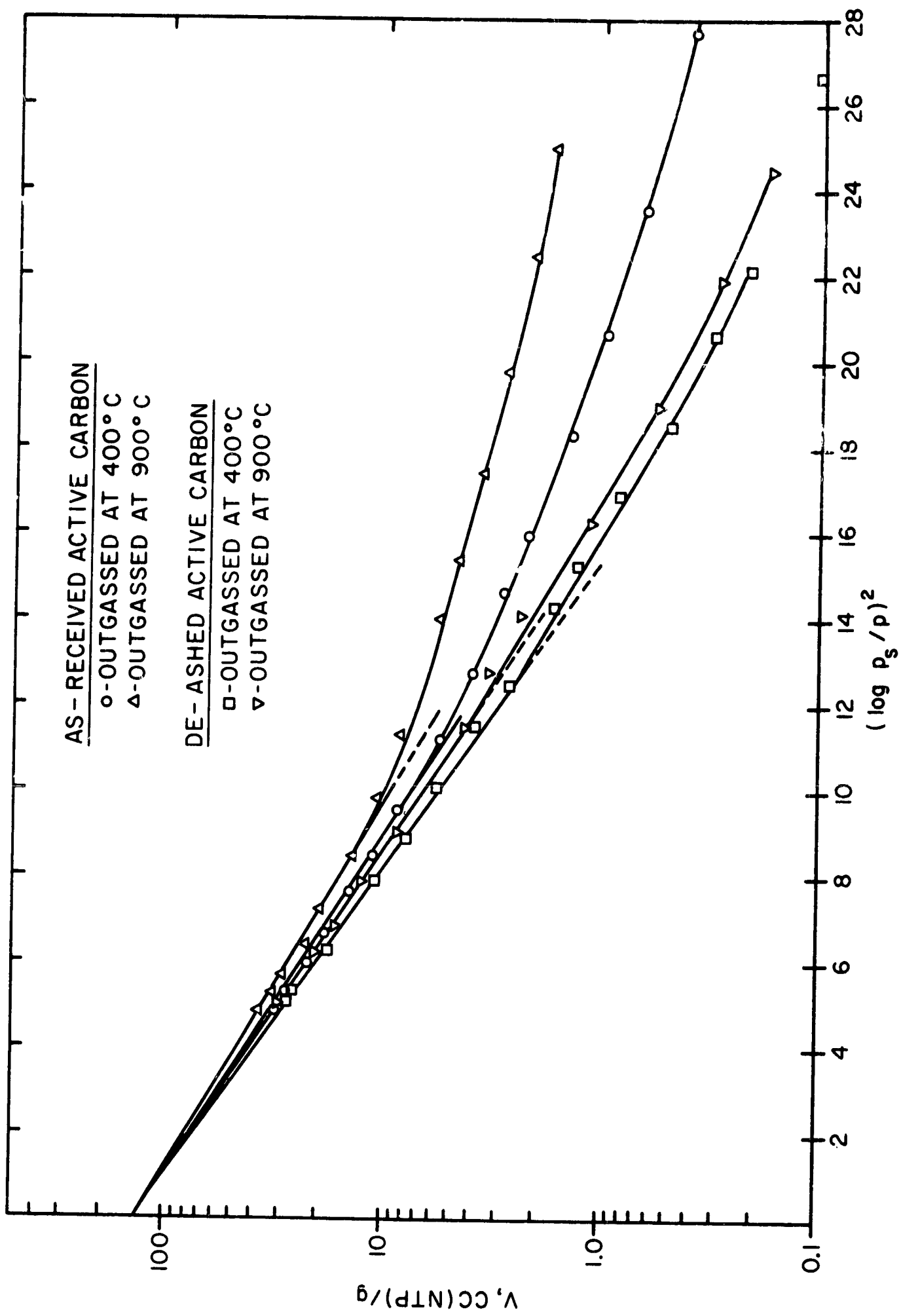


FIG. - 5

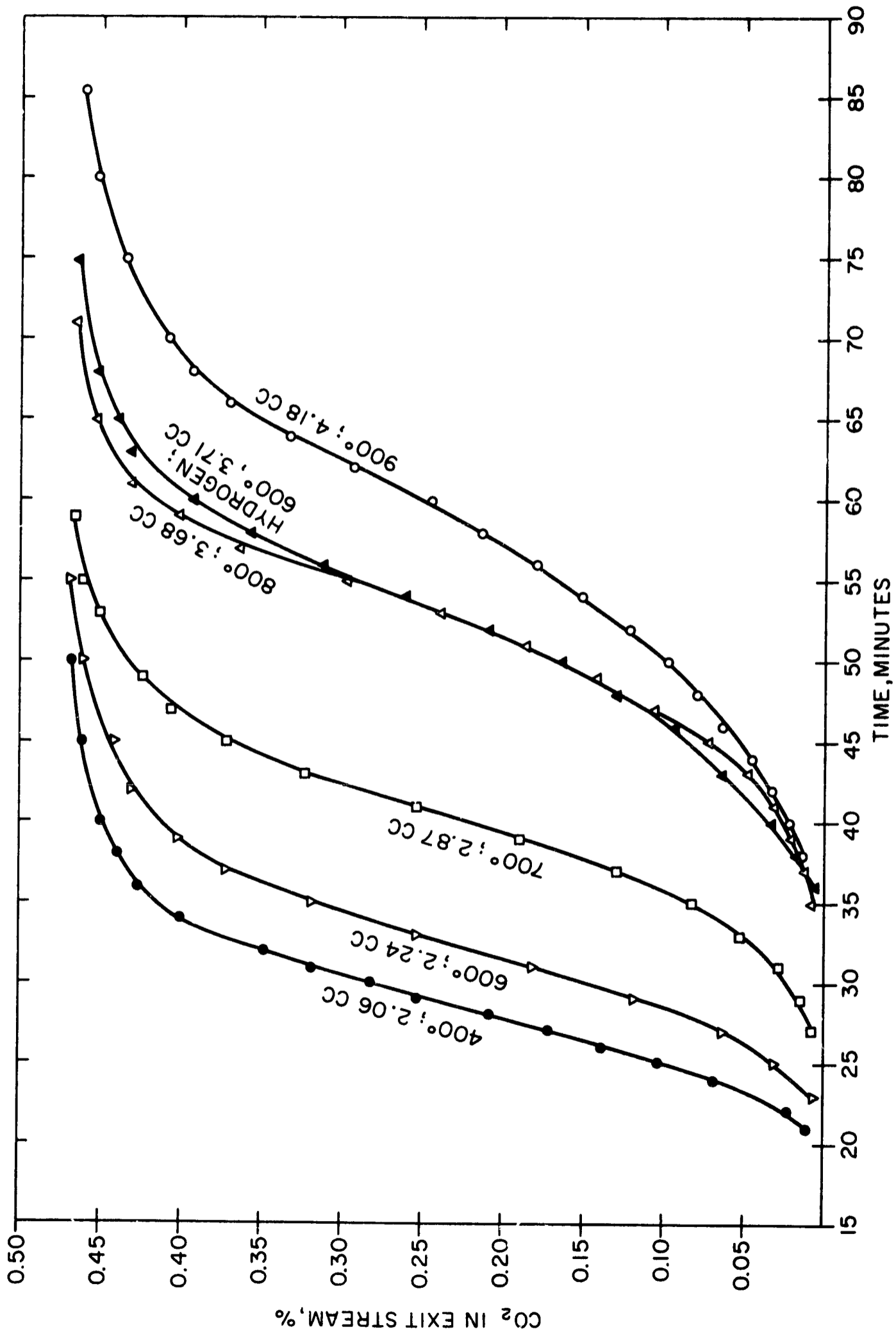


FIG. - 6

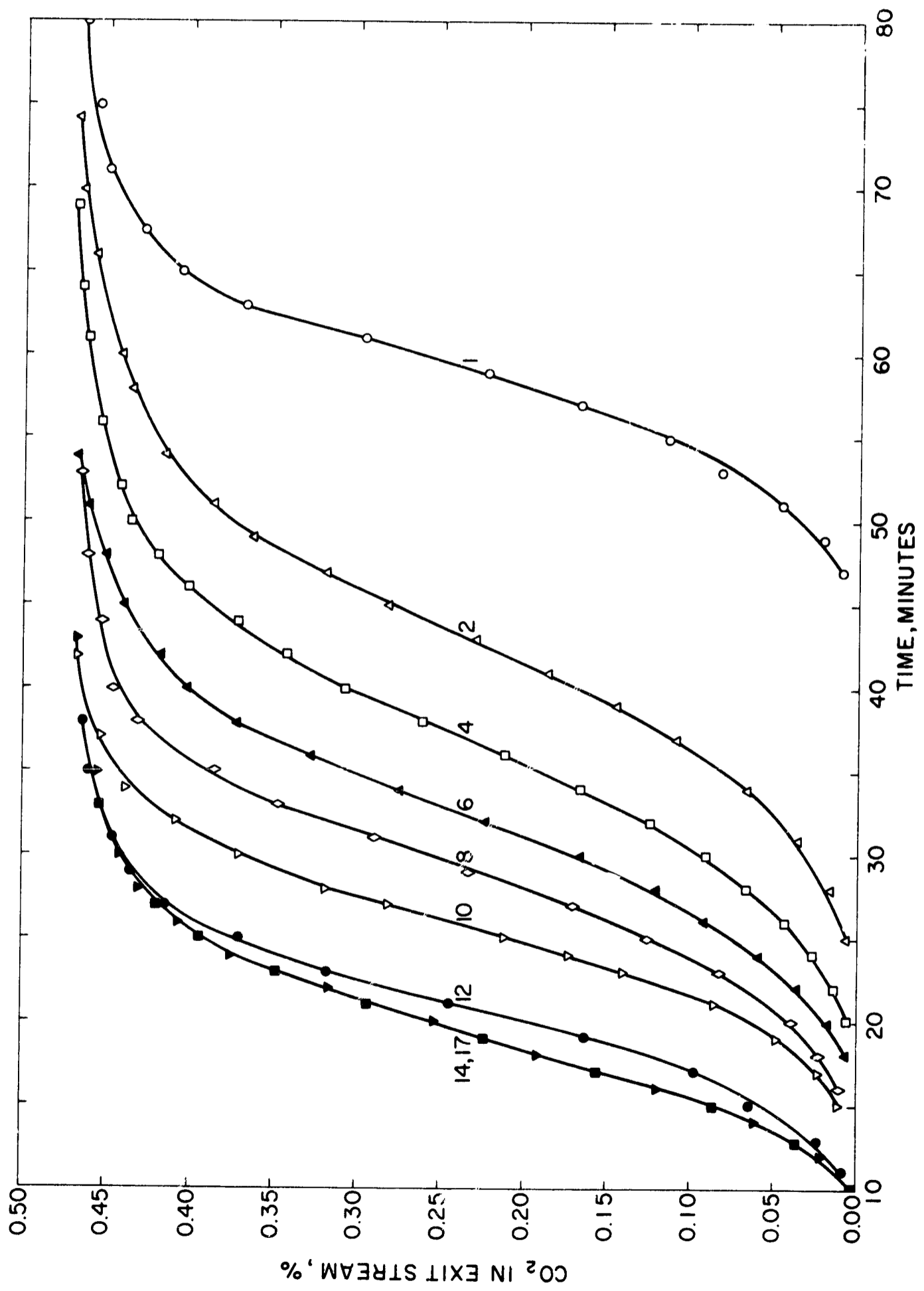


FIG. - 7

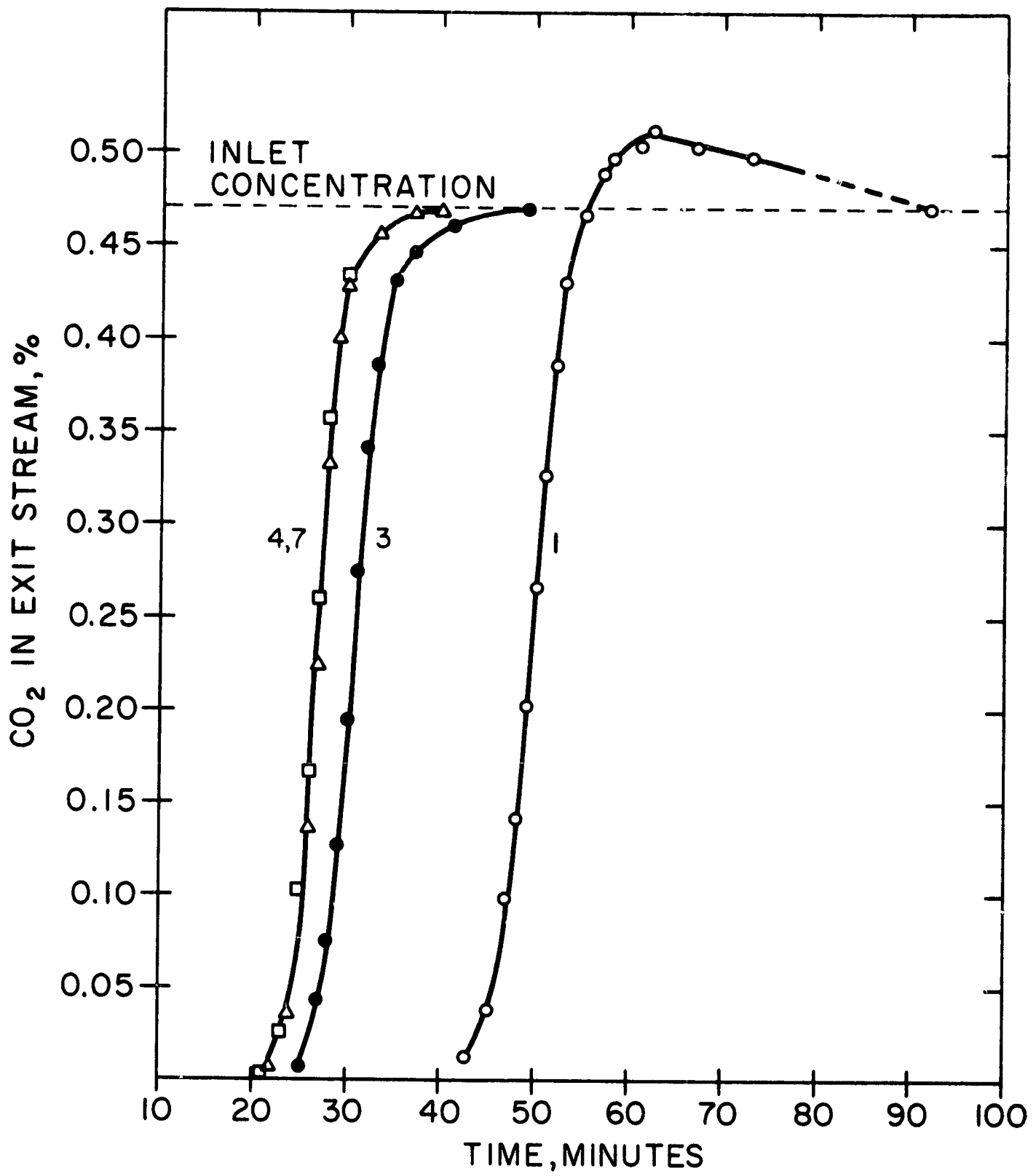


FIG. - 8

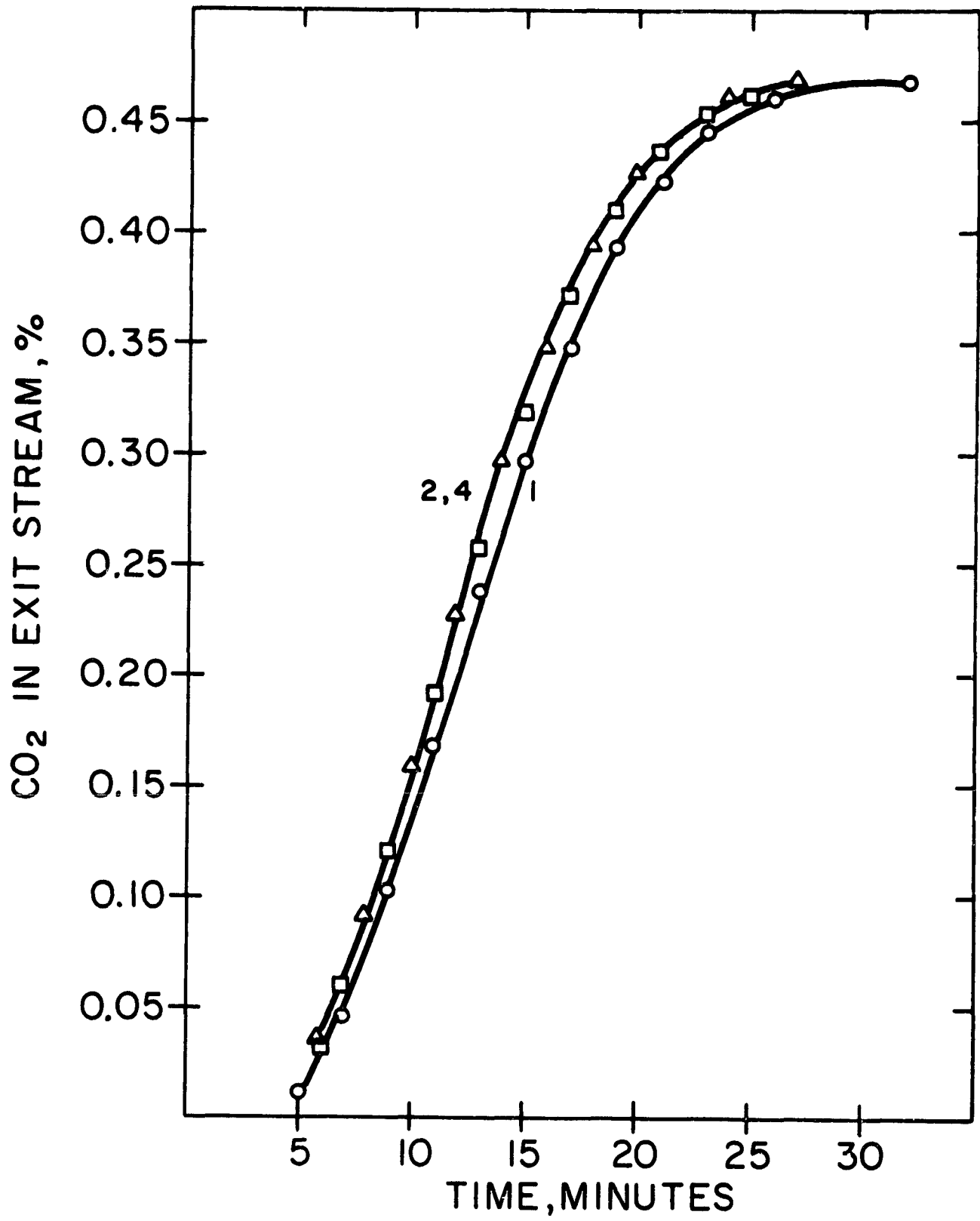


FIG. - 9

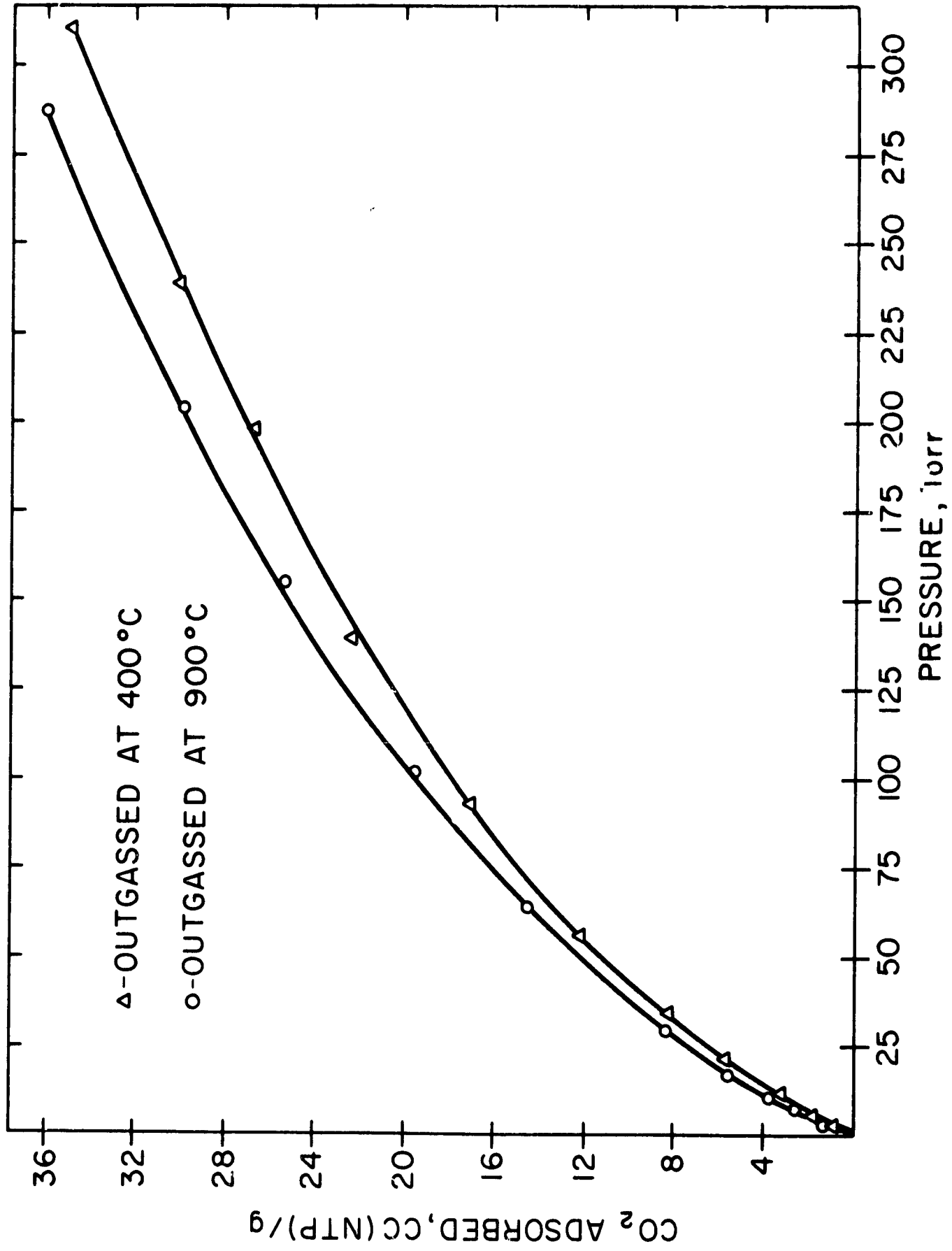


FIG. - 10